Surface damage resulting from rolling contact operating in magnetic field

Y. Iida [a, b]

T.A. Stolarski [a]

K. Sato [b]

a *Mechanical Engineering Subject Area, Brunel University, Uxbridge UB8 3PH, UK*

b *Faculty of Engineering, Department of Urban Environment Systems, Chiba University, 1-33 Yayoi, Inage, Chiba 263 8522, Japan*

Abstract

This paper describes the effects of magnetic field in rolling contact tests of steel by using a two-disc configuration and the investigation of its mechanism.

In the tests, two contact conditions, pure rolling and rolling with 10% sliding, and 1.1 and 0.4T [Tesla] of horizontal static magnetic fields created by permanent magnets are applied. Results of optical and scanning electron microscopy observations point out that finer wear particles and smoother worn surfaces are produced in the presence of magnetic field. The smoother surfaces are also confirmed by surface roughness measurements. For generation of the finer wear particles, it is considered that subsurface crack initiation point is moved toward the surface due to the magnetic field.

Wear amounts are decreased in the magnetic fields under pure rolling conditions. However, at rolling with 10% sliding, the wear amounts are increased in the magnetic fields and even finer particles and smoother surfaces are observed. Both tendencies are explained by calculating the number of cycles required to generate wear particles, which were reduced due to the magnetic field presence.

1. Introduction

Magnetic fields are generated in various mechanical and electronic devices such as motors, power generators, etc. It is important to consider tribology of their constitutive components and to understand the influence of magnetic field on their performance in order to prevent premature failure and to achieve higher energy efficiency. The main objective of this paper is to investigate the effects and mechanism by which magnetic field affects the operation of a model rolling contact through surface and sub-surface observations with the aid of an optical and scanning electron microscope. For evaluation of the mechanism, contact mechanics theory and magnetism theory were applied.

The effect of magnetic field on friction and wear processes has been studied. Previous studies of wear in magnetic fields point to number of factors that should be considered:

1) Ferromagnetic wear particles behaviour due to magnetic force [1, 2].

2) Accelerated oxidation of rubbing region due to paramagnetism of oxygen [1, 2, 3].

3) Alteration of properties on rubbing interface [3, 4].

Wear in magnetic fields is assumed to be influenced by these factors. Besides, various phenomena shown in the studies are linked in a complex way with these factors. Considering the factors individually, leads to the conclusion that behaviour and the role of ferromagnetic wear particles is the only simple phenomenon. However, in magnetic fields, strongly oxidised wear particles will be more difficult factors for the contact due to paramagnetism of oxygen. Moreover, accelerated oxidation does not only affect wear particles but also rubbing surfaces. As a result, these phenomena make the mechanism complex. More specifically, highly oxidised wear particles, affected by magnetic force operating between rubbing surfaces, act both as abrasive [5] and lubricating [1, 2, 3] agent depending on their conditions. Concerning with the properties on rubbing surface, alteration in friction coefficient [2, 3] or temperature of rubbing surface [4] have been reported in experimental observations.

From the view of property of ferromagnetic materials, relationship between movement of domain walls in magnetisation process and dislocation can be suggested. Ferromagnetic materials such as Fe and Ni have domain structure composed of magnetic domains and domain walls. In magnetic field, ferromagnetic materials are magnetised by extending magnetic domains and aligning them with the field. Simultaneously, other domains reduce their areas and the borders between domain walls move during magnetisation process. Non-magnetic inclusions or defects, such as dislocations, work as resistance to the movement. For example, it can be observed as Barkhausen noise [6] and utilized for a non-destructive inspection. Additionally, Makar [7] pointed out that hysteresis loop of steel is changed by loading. From these results, it is confirmed that magnetic fields affect mechanical properties of ferromagnetic materials. However, these effects due to magnetic field have not been explained in connection with magnetisation process of ferromagnetic materials as a whole.

The main objective of this study is to investigate the effects and mechanisms by which the magnetic field affects the operation of a model rolling contact. Another objective is to evaluate the mechanism of crack initiation under the influence of the magnetic field. These objectives are accomplished by using contact mechanics theory, magnetism theory, and surface and sub-surface observations with the aid of a scanning electron microscope.

2. Experimental conditions

Experiments in this study are carried out in two-disc rolling contact test apparatus shown in Figure 1. To

investigate the effect of horizontal magnetic field on rolling contact fatigue, permanent magnets are attached to the equipment. A large driving disc connected to the prime mover drives the test disc. By turning the driven disc about its vertical axis a degree of slip can be introduced into the contact.

To evaluate the effect of magnetic field on rolling contact fatigue, a disc with 50mm diameter and thickness of 4mm made from EN1A free cutting steel is used as a driven disc. Its hardness was about 160 HV. The driving disc has 150mm diameter and 16mm thickness and is made of ground and hardened EN40B steel containing 3% wt% Cr. Its hardness was about 615 HV. Chemical composition and mechanical properties of both discs are shown in Table 1 and 2. All experiments were performed in unlubricated ambient conditions. Prior to any test, surface roughness measurements and optical microscopy observations were conducted and initial inspection of the surface was carried out. Before each test, the surface of the driving disc was finished with a fine abrasive paper and the surfaces of driven discs were used as machined. The resultant roughnesses R_a of driving and driven discs were about 0.08μm and 0.10μm respectively. Discs were cleaned with acetone before the tests.

The contact load was kept fixed during the duration of the test. The experiments were conducted under P=150N of normal load by using dead weights. According to Hertz's theory, width of the contact area a and the maximum contact pressure p_0 are 89.7μm and 266.3MPa respectively. In addition, at condition of μ=0, the maximum shear strain-energy is 86.7MPa at depth 63.2μm.

Rotational speed and the slip ratio were kept fixed during the duration of a test. The driving disc was connected to a variable speed electric motor via a coupling. Rotational speed of driven disc was set to 450 rpm.

In order to introduce slip into the contact, the driven disc was turned about its vertical axis as shown in Figure 2 (a). By turning the driven disc, linear velocity of the driven disc, imparted on it by the driving disc v_1, (Figure 2 (b)), is resolved into v_{21} and v_{22}. Assuming that the velocities are transmitted without any loss, their relations are expressed as follows;

$$v_1^2 = v_{21}^2 + v_{22}^2 \qquad (1)$$

$$v_{22}\big/v_{21} = \tan\phi \qquad (2)$$

By using the angle ϕ as ($\tan^{-1}$ (1/10)) equal to 5.71°, 10% of slip ratio is introduced into the contact. In the present study, the slip ratio was set to 0 (pure rolling) and 10% (rolling with sliding).

To create magnetic fields, two types of permanent magnets were used with magnetic fields of 1.1 and 0.4 Tesla (T). Magnetisation created nearby the contact surface was perpendicular and the magnetic densities for the two types of permanent magnets are 0.08T and 0.02T. Therefore, magnetisation of specimen was

considered to be in a weak domain wall displacement status, as the displacement was probably placed under restraint by inclusions or dislocations.

All experiments were conducted in laboratory air environment at a temperature of about 20°C. The load and speed were kept fixed during the duration of the test. To evaluate the effect of magnetic field, the following were monitored;

(1) Weight loss of the driven disc

(2) Surface roughness R_a

(3) Appearance of disc surface and accumulation of wear particles

Prior to any test, the weight and surface roughness of the driven disc were measured and recorded. Surface roughness measurements were conducted and the initial inspection of the surface was carried out. The disc was then mounted into the test apparatus. Weight loss and surface roughness measurements were made after cleaning the disc. The weight loss measurements were carried out at regular intervals by difference in the weight of the driven disc before and after the test. Wear particles generated during the test and stuck on the surface of the disc were carefully removed by ultrasonic cleaning.

The surface roughness measurements during this study were performed on a Rank Taylor Hobson instrument (Stylus Profilometer) with a stepped motor.

The Scanning Electron Microscope (SEM) used for surface observations in this study was Cambridge S250. The image can be magnified in the range of x10 to x100, 000 and provide a much greater depth of field comparing to the optical microscope.

3. Experimental results

3.1. Pure rolling tests

Accumulated weight losses of the driven discs in pure rolling tests are shown in Figure 3. They are proportional to the number of cycles when magnetic field was absent. Above 4×10^6 cycles, total weight loss was over 1000mg. On the other hand, weight loss in magnetic fields was lower under two magnetic field conditions used. They increased in proportion to the number of cycles until around 2×10^6 cycles, a similar trend as for the absence of magnetic fields. However, this trend reached plateau after that number of cycles. The trend was especially noticeable for magnetic fields of 1.1T. The amount of wear in magnetic fields was 287mg at even 5.0×10^6 cycles. From these results, it can be stated that the wear amount resulting from rolling contact fatigue was reduced due to horizontal magnetic field effect.

Surface roughness of the driven disc was also lower in magnetic fields. As shown in Figure 4, without magnetic fields, R_a value was raised from 0.1μm to approximately 0.5μm after 6×10^5 cycles. After that, it

varied between about 0.4 to 0.6μm. In contrast, in the magnetic fields, the roughness, after 6×10^5 cycles, was increased to about only 0.3 μm. After that, the R_a value was further lowered to about 0.1μm.

Surface observations of driven disc under the SEM are shown in Figures 5(a) and (b). The effect of magnetic field on surface roughness was even clearer in SEM observations. The assembly of detached wear particles and the surface after testing without magnetic field are shown in Figure 5(c). The flat and flake shaped particles are considered to suggest that a crack was initiated at subsurface region. In addition, the thickness of larger particles was estimated to be, approximately, 20-30μm and the surface asperity was corresponding to the particles' thickness. Contrary to this, finer wear particles and smoother surface were produced due to the presence of a horizontal magnetic field as seen in Figure 5(d). The thickness of these particles was not more than 10μm. Thus, it can be said that the wear particles generated in rolling contact became finer due to the effect of a horizontal magnetic field. Therefore, when the thickness of wear particles is assumed to correspond to the subsurface location of crack initiation point, it is apparent that that point was moved towards the surface. Also, the effect of magnetic field presence is reflected in particles' size.

3.2. Rolling with sliding

As shown in Figure 6, accumulated weight losses of discs in tests with 10% sliding and without magnetic field were proportional to the number of cycles; the same trend as that for pure rolling tests. With horizontal magnetic fields, although wear amounts were lowered by magnetic fields at pure rolling, weight losses at rolling with sliding were higher than that recorded without magnetic field. This trend was especially noticeable at B=1.1T.

Figure 7 shows comparison of wear rates obtained at pure rolling and rolling with sliding. The wear rate ratio of rolling with sliding to pure rolling after 1×10^6 cycles was 3.7 at B=0T, 7.6 at B=0.4T and 17.1 at B=1.1T. The results justify saying that wear under magnetic field is increased due to introduction of slip into the rolling contact.

Surface roughness values R_a at rolling with sliding, shown in Figure 8, tend to be lower under the magnetic fields; the same trend is for pure rolling. The differences in R_a values among magnetic conditions used were smaller than that for pure rolling. Specifically, comparing to pure rolling, Ra at without magnetic field was around 0.5μm and below 0.3μm for the magnetic fields. Values of R_a at rolling with sliding were in the range of 0.47-0.59 μm at without magnetic field while under the magnetic fields of 0.4T and 1.1T, R_a were in the range of 0.34-0.38μm and 0.26-0.42μm respectively.

Observations with SEM, seen in Figure 9(a) and (b) shows that surface asperities of the driven discs under 10% sliding condition are deformed plastically. The characteristic was the same at with and without

magnetic field. In contrast, same as at pure rolling conditions, the effect of magnetic field is observed in wear particles. Wear particles under the magnetic field, shown in Figures 9(c) and (d), were finer than that at without magnetic field even if the slip is introduced into the rolling. Therefore, it can be said that wear particles become finer due to the effect of magnetic fields and it is common to both, pure rolling and rolling with sliding.

4. Discussion

4.1 Rolling contact characteristics under the magnetic field

As a summary of experimental results, the following various effects of magnetic fields were observed:

1) Wear

Wear amount of the discs was decreased in pure rolling contact. However, the amount was increased under rolling with sliding conditions.

2) Surface roughness

Surface roughness values R_a of the discs were decreased and finer wear particles were produced. From the observations, wear particle thicknesses at with and without magnetic field were approximately 5μm and 20μm respectively under the pure rolling conditions.

In connection with finer wear particles generated in the presence of magnetic fields, Hiratsuka and Sasada [1] pointed out severe-mild wear transition in sliding wear with magnetic field applied. They argued that strongly oxidised wear particles, trapped on rubbing surfaces due to a magnetic force, protected rubbing surfaces and produced finer wear debris. However, the wear particles observed in the tests are considered to be different to those produced by severe-mild wear transition when the particles were generated from subsurface cracks. Therefore, it is justified to say that wear particles were generated due to subsurface crack located at the depth of about 5μm when horizontal magnetic field was applied.

From experimental results, wear amount trends were different for the two rolling conditions used. To explain the reason for the difference, by considering the thicknesses of wear particles together with wear amount, the tendencies for different contact conditions can be clarified. The total wear amount can be expressed by multiplication of number of wear particles and the size of the particle. To consider simply, it is assumed that wear particles in this study are generated in fixed thickness defined by the magnetic condition and the size of the particles depends on their thickness. Hence, the wear amount is determined by multiplication of the number of wear particles and the thickness of wear particle.

For instance, as shown in Figure 10, the crack initiation points are considered to correspond to the thickness of particles, which is 20μm at without and 5μm at with magnetic field. The differences in crack

initiation point locations make differences in the particles' volume and the number of cycles required to detach the particles. Specifically, when a wear particle is detached from the surface, a crack initiated at the shallower location would be thinner than that initiated in a deeper location. Thus, by evaluating the number of cycles required to detach one layer, the effect of magnetic field can be explained. The number of cycles is calculated from Equation (3).

$$n = \frac{N\rho\pi dat}{W} \qquad (3)$$

where:
n - Number of cycles to detach one layer
W - Wear amount [mg]
N - Number of cycles to wear W
ρ - specific gravity of the disc (=7.85 [mg/mm^3])
t - Thickness of wear particle
  (20[μm] at without magnetic field and 5[μm] with magnetic field)
d - Diameter of the disc (=50 [mm])
a - Thickness of the disc (=4 [mm])

By applying the equation to the measurement of accumulated weight losses, the number of cycles n under different contact and magnetic conditions, shown in Figure 11, was reduced by applying magnetic field and the trend was the same for the two different kinematical contact conditions. For pure rolling, the number of cycles n for without magnetic field was 3.8×10^5 and that for with the magnetic field was 1.2×10^5 at B=0.4T and 1.5×10^5 at 1.1T. For rolling with sliding, the number of cycles was further reduced to 2.5×10^4 at B=0.4T and 1.5×10^4 at 1.1T comparing to that for without magnetic field, 8.7×10^4. Therefore, it can be concluded that the wear particles are detached earlier due to the effect of the magnetic fields for both of the contact conditions used.

On the basis of experimental results, the effect of the magnetic field can be summarised in the following way.

(1) The cracks were initiated at the shallower point.

(2) The wear particles were detached after smaller number of load cycles.

These effects resulting from the presence of magnetic field can be explained by taking into account:

(1) Stress status and crack initiation mechanics.

(2) Magnetisation of the specimen and its energy status.

(3) Relation between the stress and the magnetisation energy statuses.

4.2.   Stress status and crack initiation mechanics

Figure 12 shows ratio of von Mises's shear strain-energy τ_R and the maximum contact pressure p_o at each depth. The maximum value of τ_R/p_o takes 0.361 and it is located at the 40μm depth. It is deeper than the depth of 20μm, which considered location of crack initiation point without magnetic field being present. In addition, at the depth of 5μm, which is the considered crack initiation point with the magnetic field, the ratio takes the minimal value of 0.321. From these results, there is no reason to suppose that a crack is initiated by the distribution of shear strain-energy.

However, considering crack initiation conditions from viewpoint of dislocation movement [9], dislocation pileup and energy accumulation are both needed to initiate a crack. Therefore, in other words, when dislocations are piled up, crack could be initiated. From this viewpoint, Chin [10] explained that at a Hertzian contact, dislocations move from the region of strong shear stress gradient towards the region of weak gradient. Applying this mechanism to the contact condition used in this study, gradient of τ_R along the depth from the surface within the contact region, obtained from Figure 12, is shown in Figure 13. From the diagram, there are discontinuous points at the depths of about 20μm, 40μm, and 80μm from the surface. Comparing it to the experimental results, at the depth of 20μm, the gradient of τ_R took the minimal value. It can be suggested that dislocations could have piled up at that point. Thus, if crack initiation is controlled by dislocation pileup and if it is determined by the gradient of τ_R, it is therefore possible that the crack initiates at the depth of 20μm. Taking into account the effect of the magnetic field, it has to be said that the gradient of τ_R was about zero at the depth of 5μm - an assumed crack initiation point.

4.3.   Magnetisation of the specimen and its energy status

Magnetic domains in ferromagnetic substance have a tendency to be divided into many thin domains to minimize the total energy when no external magnetic field exists. The total energy per area is expressed as [11]:

$$e = e_m + e_{ex} + e_a \qquad (4)$$

where:

e -   Total energy.

e_m -   Magnetostatic energy.

e_{ex} -   Exchange energy.

e_a -   Anisotropy energy.

These energies are expressed as functions of the thickness of domains defined by Equations (5) and (6) [11].

$$e_m = \frac{2I_s^2 d}{\pi^2 \mu_0} \sum_{n=1}^{\infty} \frac{1}{n^2 d} \int_0^d \sin n\left(\frac{\pi}{d}\right) x \, dx \qquad\qquad (5)$$

$$e_{ex} + e_a = \frac{1}{d}\left(\frac{JS^2 \pi^2}{a^2 N} + KNa \right) \qquad\qquad (6)$$

where:

I_s	-	Saturation magnetisation
d	-	Thickness of domain
μ_0	-	Permeability of vacuum $(=4\pi \times 10^7)$
l	-	Thickness of the crystal
J	-	Exchange integral
S	-	Total spins quantum number
a	-	Lattice constant
N	-	Number of atoms in a domain wall
K	-	Anisotropy constant

To understand the magnetic status of the driven disc, distribution of magnetic domain walls is estimated by applying these equations. For the estimation, the case of 180° domain walls are considered and the model is considered to represent the driven disc at $l=4\times10^{-3}$m of thickness. Saturation magnetisation I_s is applied as 1.93T for EN1A steel [8] and other constants are used with values of Fe, $J=2.16\times10^{-21}$, $S=1$, $N=150$ and $K=4.2\times10^4$ [11]. The thickness of the domain obtained by substituting these values to Equations (5) and (6) is 3.98×10^{-6}m. Thus, it can be conjectured that domain walls in the driven disc nearby the contact region exist at intervals of several microns when no magnetic field is applied.

Due to magnetisation, domain walls require energy in order to expand magnetic domains, therefore, turn to the magnetic field for energy, which is given by Equation (7) [11]. The value obtained for rare earth magnets by substituting I_s =1.93T for EN1A steel and H=80A/m [8] is:

$$\Delta U_m = 2I_s H \cos\theta = 2\times1.93[\text{T}] \times 80[\text{A/m}] = 309.2[\text{J/m}^3] \qquad\qquad (7)$$

where:

ΔU_m	-	Energy for magnetisation
I_s	-	Saturation magnetisation
H	-	Magnetic field
θ	-	Angle of directions between magnetic field and easy direction (assumed to $\theta=0°$)

Obtained magnetic densities nearby the contact surface for the two types of permanent magnets used are 0.08T and 0.02T. From the results, magnetisation statuses are considered to be in a weak domain wall displacement status. It means that defects, such as dislocations, restricted the

displacement of domain walls. In other words, domain walls are pinned by dislocations at the magnetisation status. At the condition, it can be guessed that domain walls move with dislocations and the energy for magnetisation stored up at domain walls is also varied with them. Therefore, it can be considered that the dislocation movement determines movement of domain walls. It can also be estimated after Makar [7] that characteristic of magnetisation of steel is influenced by the amount of carbon and stress. In consequence, it is necessary to know the behaviour of dislocations in the vicinity of the contact region.

Assuming that crack initiates at the depth of 5μm under the influence of magnetic field, it can be supposed that dislocations are piled up due to lower τ_R gradient nearby the surface. However, to initiate the crack, energy accumulation to cause plastic deformation at the point of crack initiation is needed. Considering the crack initiation model in the rolling contact under the magnetic field, dislocations nearby the contact region are supposed to be in domain wall, which are given energy due to magnetisation. Therefore, dislocations piled up at the point of crack initiation with the energy due to the energy stored up in the domain walls pinned by the dislocation.

To examine the feasibility of crack initiation model with the magnetic field, energy status at subsurface has to be estimated. Mean distance between dislocations is approximately 1-10μm at dislocation density of 10^{-10}-10^{-12} and domain wall is about 100-200b (where b is lattice constant, b=2.8x10^{-10}m for Fe) and it corresponds to 0.03-0.06μm. Schematic model for the relation between dislocations and domain walls in position is shown in Figure 14.

Magnetisation energy is accumulated in domain walls under the test conditions used and it is estimated to be about 300J/m³. Thus, assuming that a 1mm x 4mm area of domain wall lies at the depth of 5μm within the subsurface region, the energy is estimated as shown by expression (8):

$$300 \text{ [J/m}^3\text{]} \times 1 \times 10^{-3} \text{ [m]} \times 4 \times 10^{-3} \text{ [m]} \times 0.03\text{-}0.06 \times 10^{-6} \text{ [m]} = 3.6\text{-}7.2 \times 10^{-11} \text{ [J]} \qquad (8)$$

4.4.   Relation between the stress and the magnetisation energy statuses

To make a slip motion of a dislocation, activation energy that overcomes resistance for the dislocation to move is needed. Generally, the energy is supplied as external work. Additionally, the energy due to thermal vibration at lattice, called 'thermal fluctuation' can be provided as activation energy. The phenomenon is called "thermally activated process" [12].

Illustration of resistance energy is schematically shown in Figure 15. When the resistance force is compared to the height $l*$ and the range affected is compared to width $d*$, the resistance energy

for dislocation corresponds to an area of mountain-shaped curve. When external force per unit length is applied to the dislocation in the slip direction, it is expressed by Equation (9).

$$f_e = \tau_e b \qquad\qquad (9)$$

where:

f_e - External force
τ_e - Shear stress
b - Burgers vector

The activation energy obtained for f_e is equal to (a) in Figure 15 and more energy, corresponding to (b), is needed to initiate slip. The energy due to thermally activated process satisfies the gap in a probability expressed by Equation (10) [12].

$$2\exp\left(-\frac{U_o}{kT}\right)\sinh\frac{\tau_e bl^* d^*}{kT} \qquad\qquad (10)$$

where:

U_o-   Resistance energy
K - Boltzmann constant
T - Absolute temperature

The value of kT is about 4×10^{-21}J in room temperature and 1.8×10^{-20}J even if T=1300K [12]. Thus, when dislocation is slipped due to thermally activated process, it is required that there is a certain activation energy due to external work and low resistance for the motion; for instance, low resistance force or small resistance range.

Comparing the value for thermal activation process to 3.6-7.2×10^{-11}J of the energy accumulation in domain wall due to magnetisation, obtained from Equation (8), the value of the activation energy could be sufficient to activate dislocation motion, even if a very small quantity is provided.

5.   Conclusions

From experimental investigation, the effects of horizontal magnetic field on rolling contact wear were observed to be as below:

  (a) The cracks were initiated at the shallower subsurface locations.

  (b) The wear particles were detached after a smaller number of load cycles.

To consider subsurface crack initiation model, accounting for the presence of magnetic field, is proposed utilising (1) magnetisation status of the specimen and (2) dislocation status at the contact region.

(1) Magnetisation status of the specimen

Magnetisation status of the specimen nearby the contact region suggests that domain wall displacement is restricted by inclusions such as dislocations. Therefore, it can be supposed that the domain walls within contact region migrate with dislocations movement.

(2) Dislocation status within the contact region

Assuming that dislocation movement is determined by gradient of shear stress, dislocation pileup could occur close to the surface and might coincide with the shift in crack initiation point due to the magnetic field presence. Therefore, magnetic domain walls with increased energy due to magnetisation move toward the contact surface with dislocations piled up by shear stress gradient. In addition, the value of the magnetisation energy accumulated at the domain walls is large enough to compare to the energy due to thermally activated process and it is possible to consider that the magnetisation energy helps the dislocation pileup. As a result, cracks are initiated at the depth of about $5\mu m$ from the surface even if von Mises' shear strain-energy criterion at this location is not enough on its own to cause crack initiation.

References

(1) K. Hiratsuka, T. Sasada and S. Norose, "The magnetic effect on the wear of metals", Wear, Vol.110, (1986), pp. 251-261.

(2) K. Kumagai, K. Suzuki and O. Kamiya, "Study on reduction in wear due to magnetization", Wear, Vol. 162-164, (1993), pp. 196-201.

(3) H. Zaidi, L. Pan, D. Paulmier and F. Robert, "Influence of a magnetic field on the wear and friction behaviour of a nickel/XC 48 steel couple", Wear, Vol. 181-183, (1995), pp. 799-804.

(4) O. Bataineh, B. Klamecki and B.G. Koepke, "Effect of pulsed magnetic treatment on drill wear", Journal of Materials Processing Technology, Vol. 134, (2003), pp. 190-196.

(5) K. Sato, T.A. Stolarski and Y. Iida, "The effect of magnetic field on fretting wear", Wear, Vol. 241, (2000), pp. 99-108.

(6) H. Barkhausen, Z. Phys., Vol. 20, (1919), pp. 401.

(7) J.M. Makar and B.K. Tanner, "The in situ measurement of the effect of plastic deformation on the magnetic properties of steel: Part I – Hysteresis loops and magnetostriction", Journal of Magnetism and Magnetic Materials, Vol. 184, (1998), pp. 193-208.

(8) "The mechanical and physical properties of the British standard EN steels", Steel user service British iron and steel research association, (1964), Pergamon press.

(9) H. Czichos, "Tribology", (1978), Elsevier scientific publishing company

(10) K.J. Chin, H. Zaidi, M.T. Nguyen and P.O. Renault, "Tribological behaviour and surface analysis of magnetized sliding contact XC 48 steel/XC 48 steel", Wear, Vol. 250, (2001), pp. 470-476.

(11) S. Chikazumi, "Physics of magnetism", John Wiley & Sons, Inc. (1964)

(12) O. Izumi, "Atomism for material strength", (1985) The Japan Institute of Metals

List of tables

List of figures

Table 1 Composition of specimens [wt%] [8]

	C	Si	Mn	S	P	Ni	Cr	Mo
EN1A	0.05-0.15	0.10max	0.80-1.20	0.20-0.30	0.070max	-	-	-
EN40B	0.10-0.20	0.10-0.35	0.40-0.65	0.050max	0.050max	0.40max	2.90-3.50	0.40-0.70

Table 2 Mechanical properties of specimens [8]

	Young's modulus [GPa]	Poisson's ratio	Yield strength [MPa]	Tensile strength [MPa]
EN1A	203	0.28	243	394
EN40B	205	0.30	516	684

Figure 1 Two-disc rolling contact test apparatus

$\phi = \tan^{-1}(1/10) = 5.71^{\circ}$

(a)   (b)

Figure 2 Geometry of pure rolling and rolling with sliding
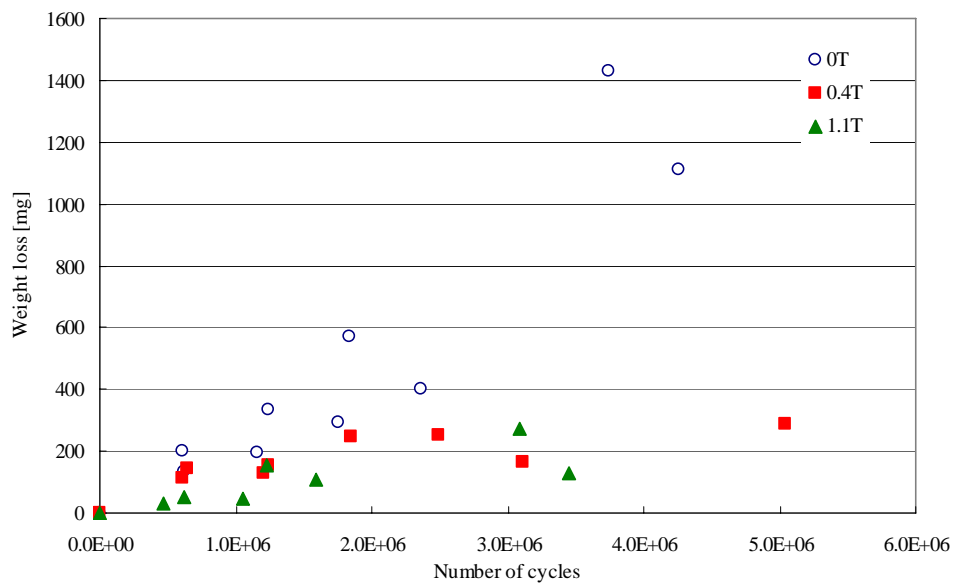
Figure 3 Accumulated weight losses of mild steel discs (Pure Rolling)
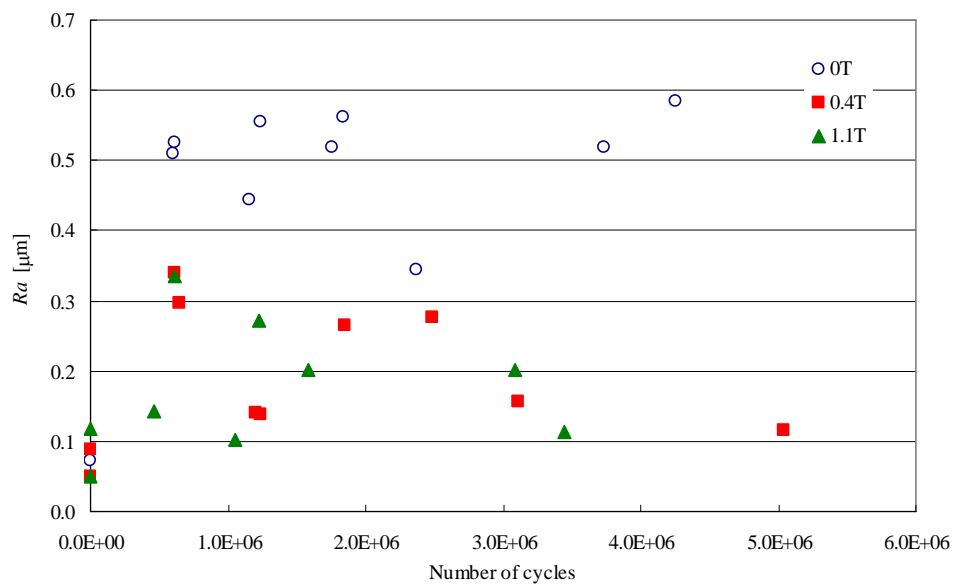
Figure 4 Surface roughness of mild steel discs (Pure Rolling)

(a) Surface, *B*=0T,

(b) Surface, *B*=0.4T

(c) Wear particles, *B*=0T

(d) Wear particles, *B*=0.4T
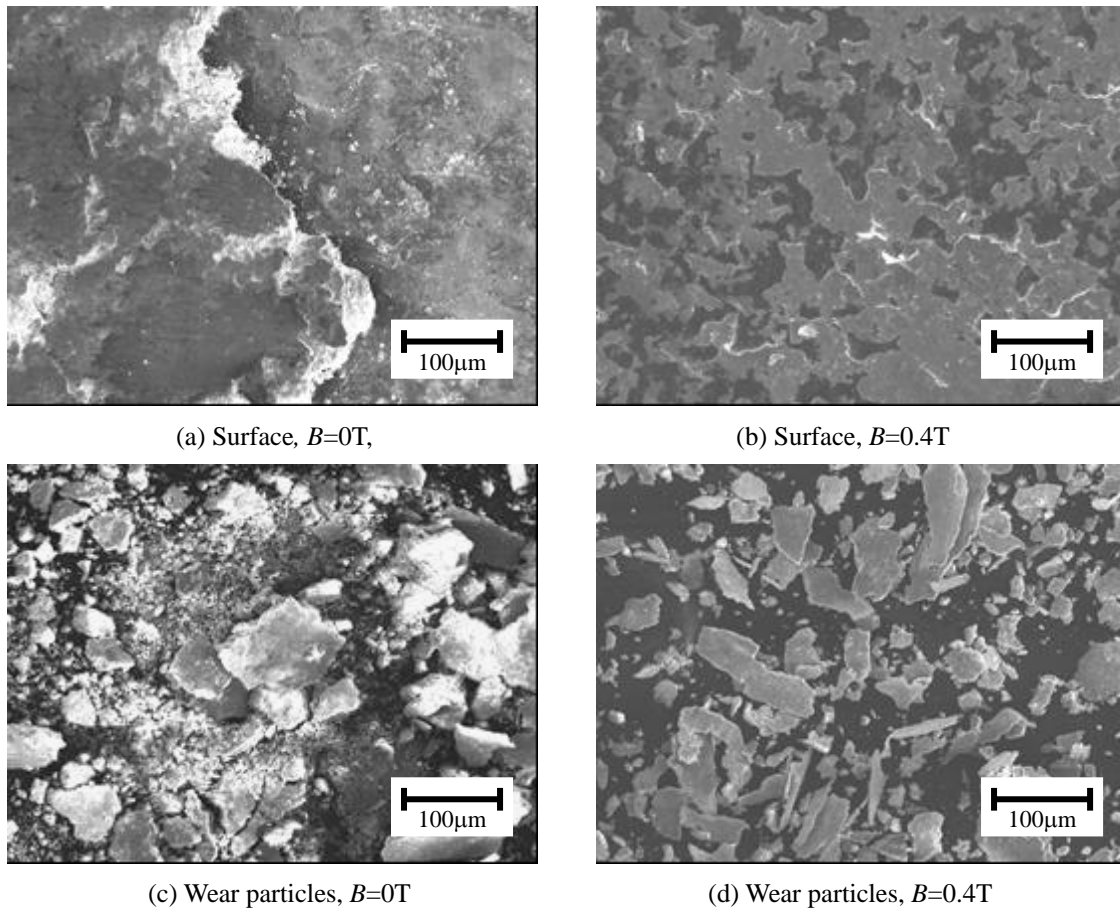
Figure 5 Surface and wear particles observations of mild steel discs (Pure Rolling)
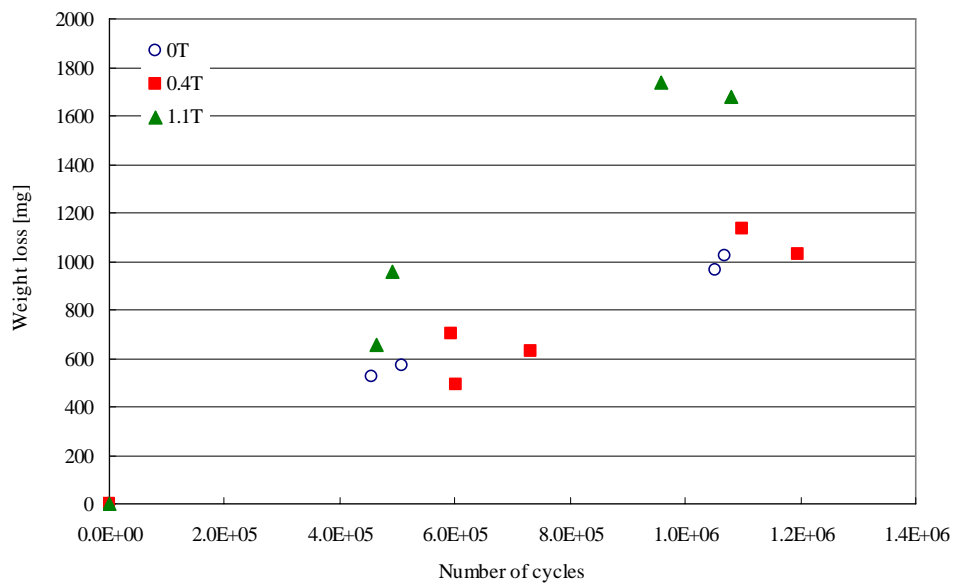
Figure 6 Accumulated weight losses of mild steel discs (Rolling with Sliding)
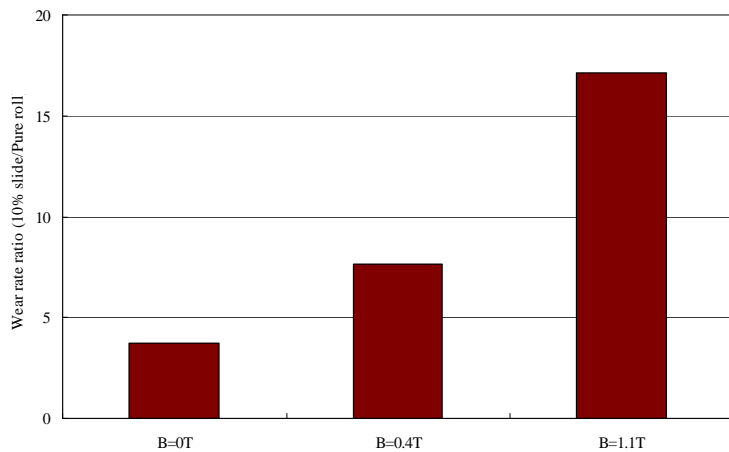
Figure 7 Wear rate ratios for pure rolling and with rolling with sliding.
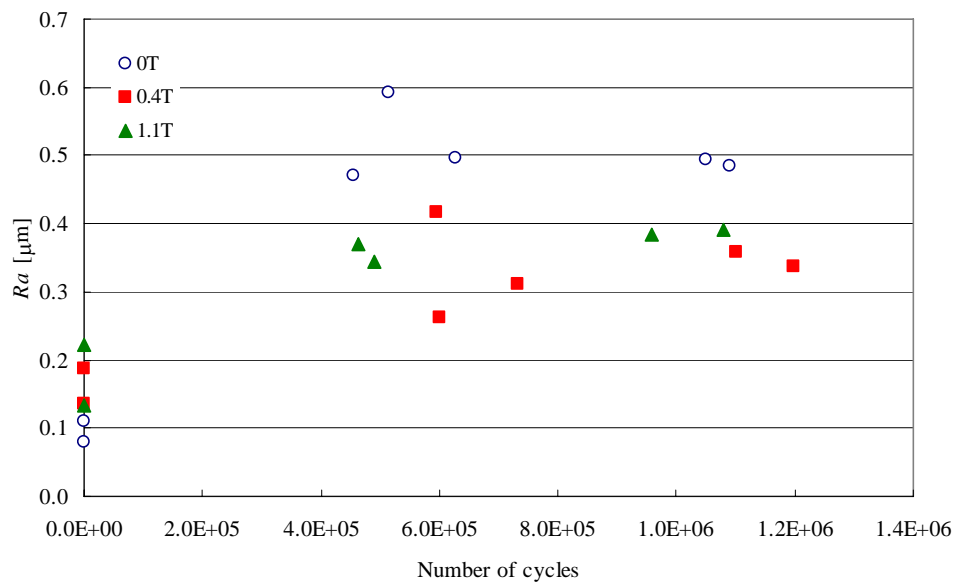
Figure 8 Surface roughness of mild steel discs (Rolling with Sliding)

(a) Surface, *B*=0T,

(b) Surface, *B*=0.4T

(c) Wear particles, *B*=0T

(d) Wear particles, *B*=0.4T
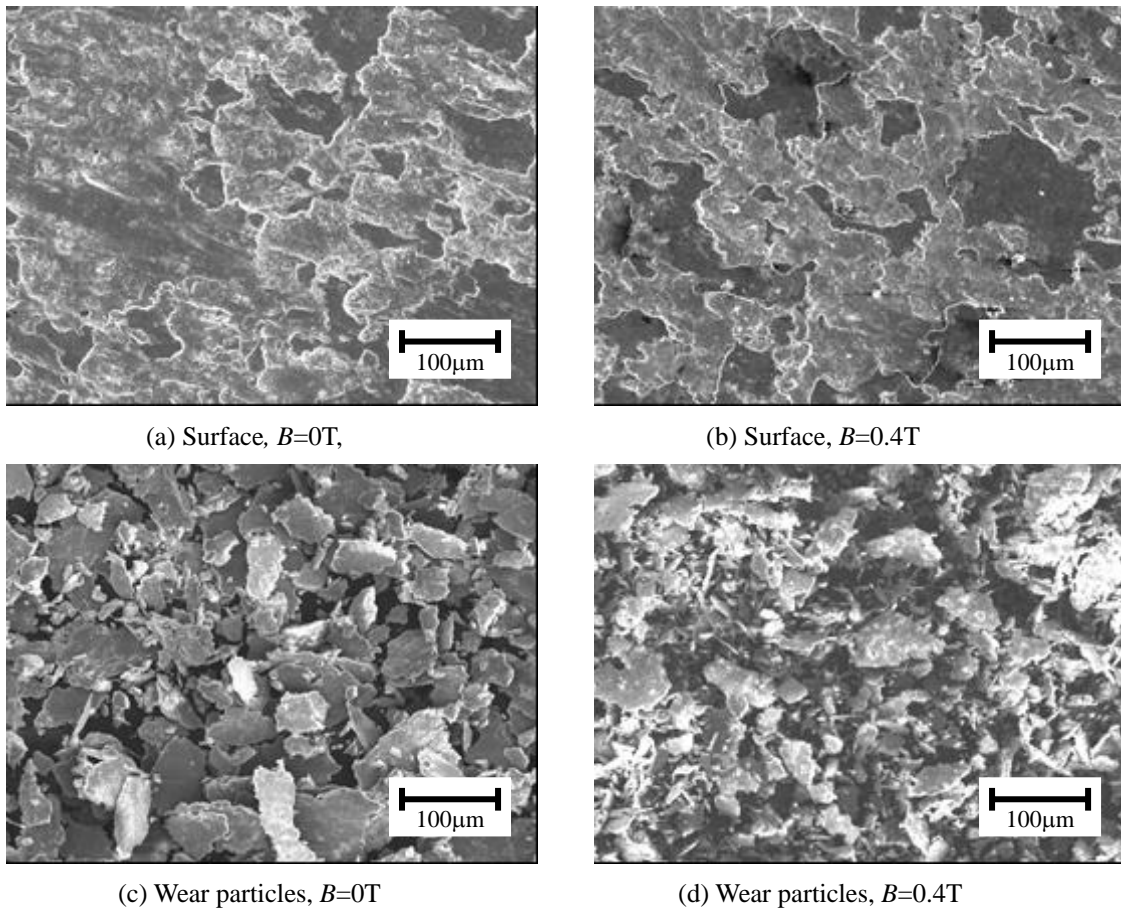
Figure 9 Surface and wear particles observations of mild steel discs (Rolling with Sliding)
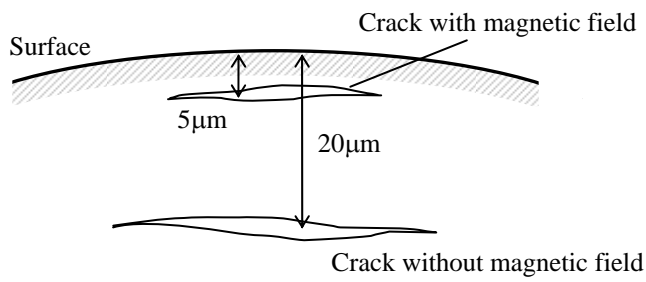
Figure 10 Difference of crack initiation points at subsurface with and without magnetic field
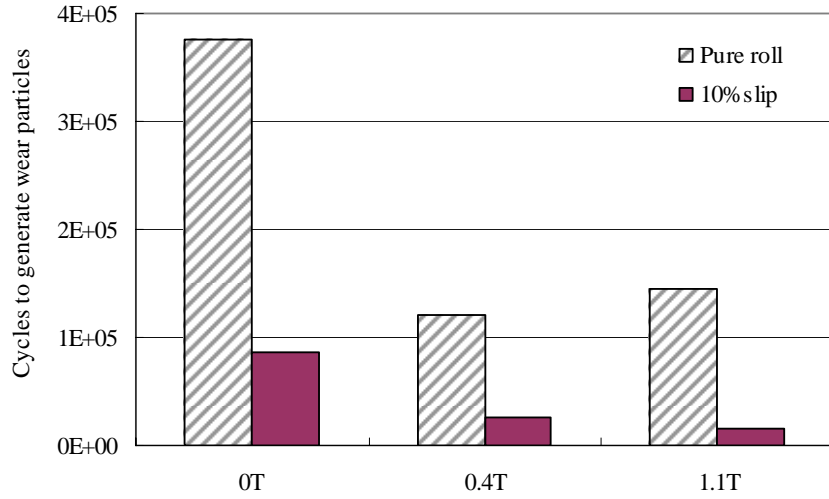
Figure 11 Cycles to generate wear particles with and without magnetic field
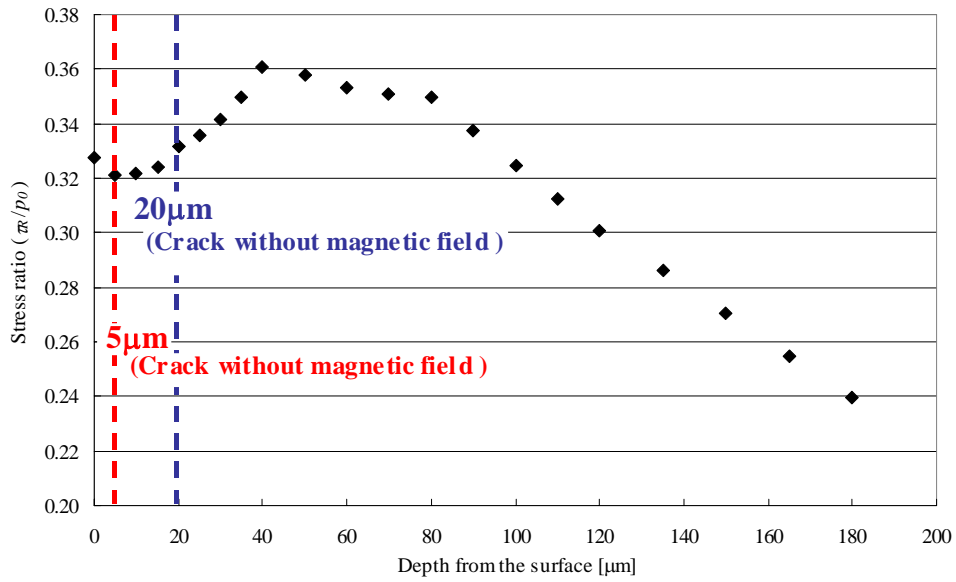
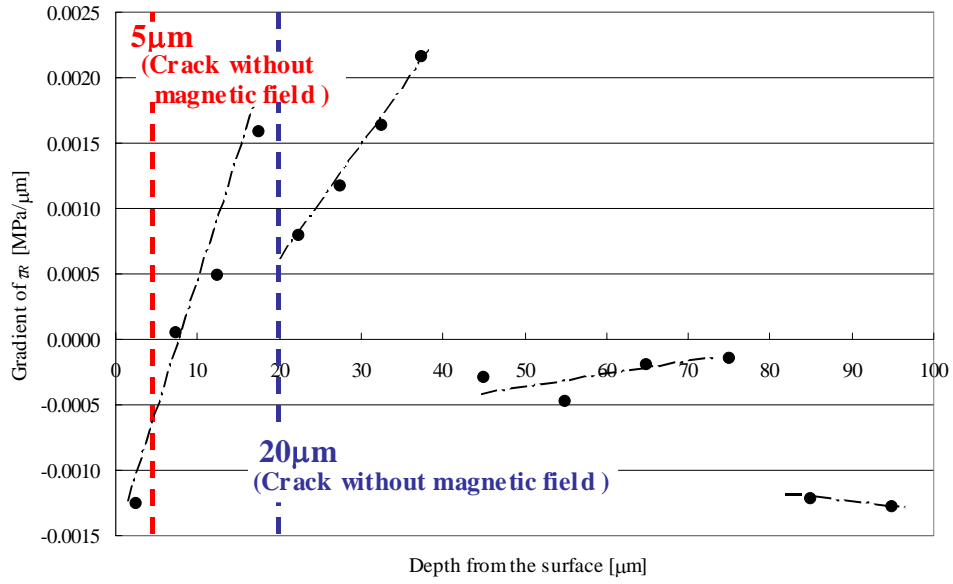Figure 12 Stress distributions of τ_R/p_0 at subsurface and crack initiation points

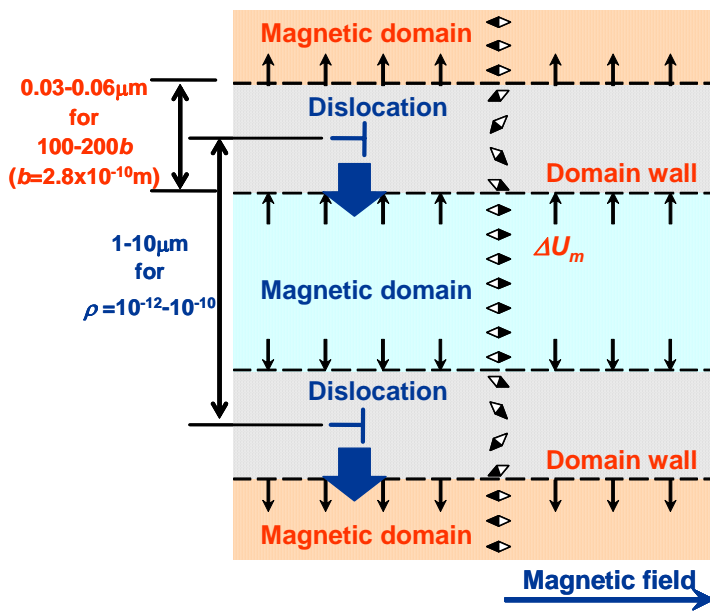Figure 13 Maximum shear stress gradients at contact region

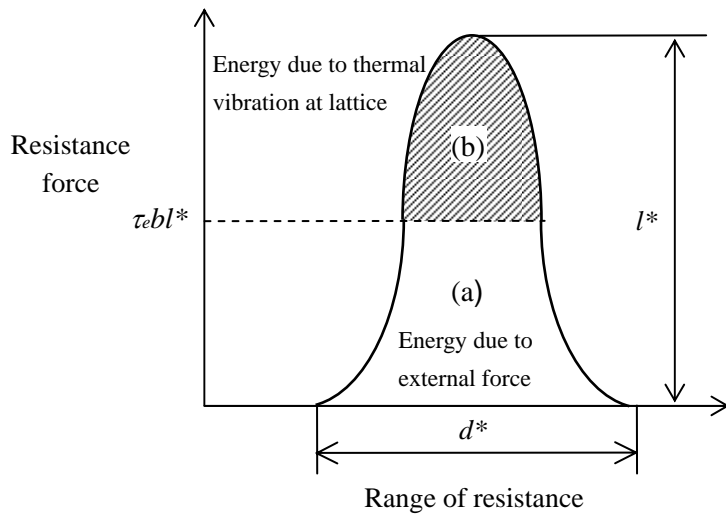Figure 14 Relation of dislocations and domain walls in position

Figure 15 Resistance energy for dislocation [12]